



Synthesis and mesomorphic properties of quinoline-8-yl-4-((4-n-alkoxy benzylidene) amino) benzoate: The effect of linkage group

Vinay. S. Sharma, Rajesh H. Vekariya, Anuj. S. Sharma & R. B. Patel

To cite this article: Vinay. S. Sharma, Rajesh H. Vekariya, Anuj. S. Sharma & R. B. Patel (2017): Synthesis and mesomorphic properties of quinoline-8-yl-4-((4-n-alkoxy benzylidene) amino) benzoate: The effect of linkage group, *Molecular Crystals and Liquid Crystals*, DOI: 10.1080/15421406.2017.1358006

To link to this article: <http://dx.doi.org/10.1080/15421406.2017.1358006>



Published online: 12 Sep 2017.



Submit your article to this journal [↗](#)



Article views: 7



View related articles [↗](#)



View Crossmark data [↗](#)



Synthesis and mesomorphic properties of quinoline-8-yl-4-((4-n-alkoxy benzylidene) amino) benzoate: The effect of linkage group

Vinay. S. Sharma^a, Rajesh H. Vekariya^b, Anuj. S. Sharma^b, and R. B. Patel^a

^aChemistry Department, K.K. Shah Jarodwala Maninagar Science College, Gujarat University, Ahmedabad, Gujarat, India; ^bDepartment of Chemistry, School of Science, Gujarat University, Ahmedabad, Gujarat India

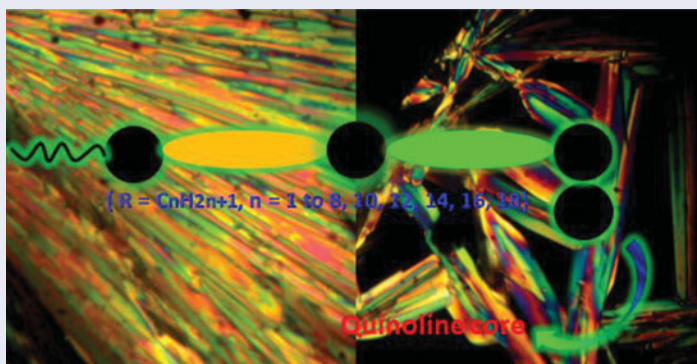
ABSTRACT

A new homologous series viz. quinoline-8-yl-4-((4-n-alkoxy benzylidene) amino) benzoate based on two central linking groups have been designed and characterised by elemental analyses and spectroscopic techniques such as Fourier transform infrared [FT-IR] and proton-magnetic resonance magnetic resonance [¹H NMR] spectroscopy. The mesomorphic properties of these compounds were observed by polarizing optical light microscopy (POM) and confirmed by differential scanning calorimetry (DSC). All synthesized compounds displayed LC property except first two homologue. The lower homologues (n = 4 to 8) display SmA and SmC phase while, in higher homologues (n = 10 to 18) SmC and nematic phase were seen in heating and cooling condition.

KEYWORDS

Mesomorphic; nematic; smectic; thermotropic

GRAPHICAL ABSTRACT



1. Introduction

Suitable magnitudes of anisotropic forces of intermolecular attractions as a consequence of molecular rigidity and flexibility can favorably induce a physically distinct state of a substance between the crystalline solid and the isotropic liquid states, called the liquid crystal state [1–3]. Normally structures consist of two or more rings (aromatic, homocyclic or

CONTACT Vinay. S. Sharma  vinaysharma3836@gmail.com  Chemistry Department, K.K. Shah Jarodwala Maninagar Science College, Gujarat University, Ahmedabad, Gujarat, 380008, India; Rajesh H. Vekariya  rajeshvekariya007@gmail.com  Department of Chemistry, School of Science, Gujarat University, Ahmedabad, 380009, Gujarat, India.

Color versions of one or more of the figures in the article can be found online at www.tandfonline.com/gmcl.

© 2017 Taylor & Francis Group, LLC

heterocyclic) and central linking part encompass the rigidity and presence of terminal groups act as the flexible part of the molecule. The introduction of aromatic groups such as biphenyl or naphthyl ring has been widely studied because they give rise to very stable mesophases and allow the introduction of substituents into different positions leading to modification of the liquid crystalline property [4–5].

In the last few years, heterocyclic liquid crystals have been of great scientific interest. The presences of heterocyclic as a part of the core provide perpendicular dipolar moments as well as polarizable structures, which can lead to SmC phases [6]. 2, 6-disubstituted quinoline based liquid crystalline compounds were synthesized and their mesogenic properties were reported in literature [7–9]. Lin et al. reported first heterocyclic liquid crystalline molecules containing 3,7-disubstituted quinoline displayed widest range of SmC phase [10]. Zanardi et al. reported 2-phenylquinolines with alkyl or alkoxy substituents in positions at 6 and 4' side which displayed nematic mesophase [11]. Previously, Chia et al. reported a regioselective addition of organometallic reagents to 1-acylpyridinium and 1-acylquinolinium salts to prepare nitrogen containing heteroaryl mesogenic compounds [12–14]. Chia et al. reported two liquid crystalline series based on 6-methoxy quinolines derivatives [15]. Bhoja et al. reported non-mesogenic behaviour of 8-(4'-n-alkoxy benzoyloxy) quinolines series which consisted twelve homologous [16]. Binnemans and his group reported ionic liquid crystals based on quinolinium and isoquinoline derivatives [17]. The numbers of homologous series contain two central groups; azomethine ($-\text{CH}=\text{N}-$) and ester ($-\text{COO}-$) linkage groups [18–21].

Continuing our work on the liquid crystal possibilities of the quinoline system, we have synthesized and studied the LCs properties of newly series contain imine ($-\text{CH}=\text{N}-$) and ester ($-\text{COO}-$) as a central linkage group and presence of quinoline core which is isoelectronic and isogeometric with respect to naphthalene core systems.

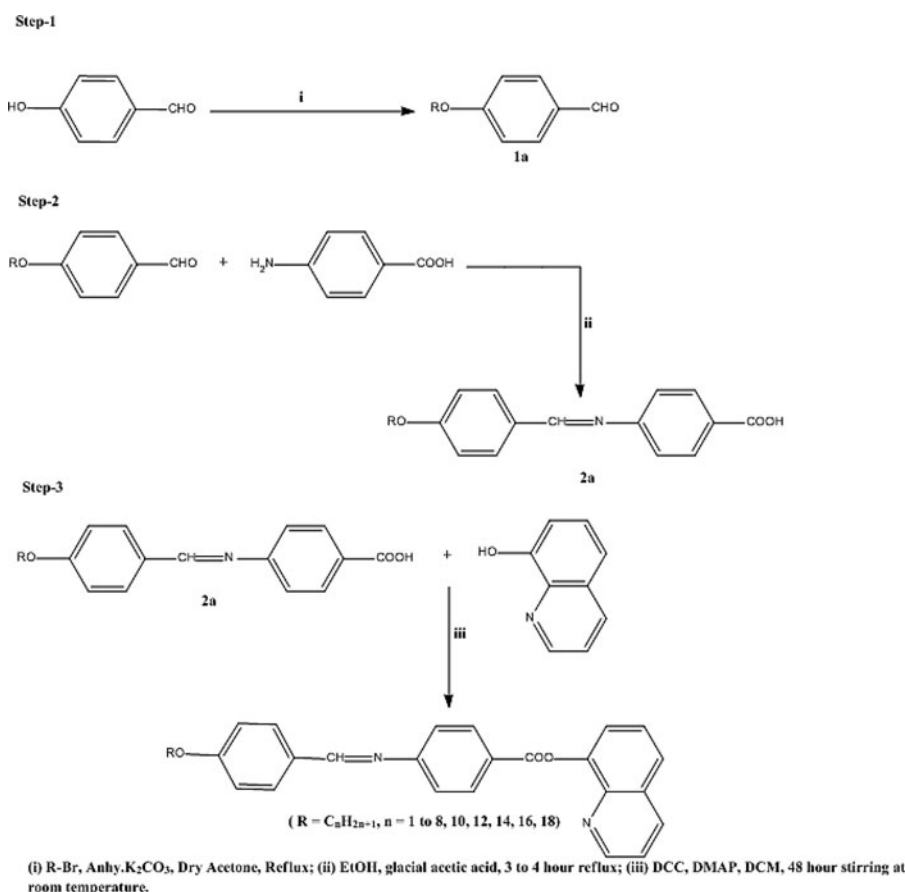
2. Experimental

2.1. Materials

For present synthesized homologous series required materials: 4-hydroxy benzaldehyde, 4-amino benzoic acid purchased from (S.R.L, Mumbai), 8-hydroxy quinoline purchased from (Sigma Aldrich). Anhydrous K_2CO_3 was purchased from (Finar Chemical, Ahmedabad), N, N-dimethyl amino pyridine (DMAP) and Dicyclohexylcarbodiimide (DCC) were purchased from (Fluka Chemie, Switzerland). Alkyl bromides (R-Br) were purchased from S.R.L. Chemicals (Mumbai). All solvents were dried and purified by standard method prior to use.

2.2. Measurements

Melting points were taken on Opti-Melt (Automated melting point system). The FT-IR spectra were recorded as KBr pellet on Shimadzu in the range of $3800\text{--}600\text{ cm}^{-1}$. Microanalysis was performed on Perkin-Elmer PE 2400 CHN analyser. The texture images were studied on a trinocular optical polarising microscope (POM) equipped with a heating plate and digital camera. ^1H NMR spectra was recorded on a 400 MHz in Bruker Advance 400 in the range of 0.5 ppm – 16 ppm using CDCl_3 as solvent. The phase transition temperatures were measured using Shimadzu DSC-60 at heating and cooling rates of $10^\circ\text{C min}^{-1}$. Texture image of nematic phase were determined by miscibility method. Thermodynamic quantities enthalpy (ΔH) and entropy ($\Delta S = \Delta H/T$) are qualitatively discussed. For the POM study, novel synthesized compound is sandwiched between glass slide and cover slip and heating and cooling rate is (2°C /min) respectively.



Scheme 1. Synthetic route of series-1.

2.3. Synthesis

4-*n*-alkoxy benzaldehyde (A) was prepared by reported method [22]. 4-((4-alkoxy benzylidene) amino) benzoic acid (B) was prepared by usual established method [23]. Esters (C₁ to C₈, C₁₀, C₁₂, C₁₄, C₁₆, C₁₈) were synthesized by a reported method in literature [24]. Thus, the synthesized target compounds were filtered, washed, dried and purified till constant transition temperatures is obtain by using an optical polarizing microscope (POM) equipped with a heating stage. The synthetic route to a series is mentioned in Scheme 1.

2.3.1. Synthesis of 4-*n*-alkoxy benzaldehyde (A)

4-*n*-alkoxy benzaldehyde (A) was synthesized by refluxing the mixture of 4-hydroxy benzaldehyde (1 equiv.) with corresponding *n*-alkyl bromide (R-Br) (1 equiv.) in presence of anhydrous K₂CO₃ (1.2 equiv.) in dry acetone as a solvent [22].

2.3.2. 4-((4-alkoxy benzylidene) amino) benzoic acid (B)

4-((4-alkoxy benzylidene) amino) benzoic acid was prepared by refluxing the mixture of (A) and 4-amino benzoic acid at 3 to 4 hours in presence of ethanol and few drops of acetic acid [23]. The resultant mixture was filtered, dried, and purified by column chromatography which was confirmed by IR and ¹H NMR analysis.

2.3.3. Synthesis of quinoline-8-yl-4-((4-*n*-alkoxy benzylidene) amino) benzoate (C)

Quinoline-8-yl-4-((4-*n*-alkoxy benzylidene) amino) benzoate (C) was prepared by esterification of (B) and 8-hydroxy quinoline by usual established method reported in literature [33]. The appropriate (B) (2.02 mmol) and 8-hydroxy quinoline (C) (0.246 g, 2.02 mmol), dicyclohexylcarbodiimide (DCC) (0.457 g, 2.22 mmol) and dimethylaminopyridine (DMAP) in catalytic amount (0.002 g, 0.2 mmol) in dry CH₂Cl₂ (DCM) (40 ml) was stirred at room temperature for 48 h. The resultant crude product was purified by column chromatography on silica gel eluting with dichloromethane: methanol and recrystallization from chloroform until the constant transition temperatures were observed.

2.3.4. Reaction Scheme

2.3.5. Analytical data

Compound (2a₁): FT-IR (KBr) in cm⁻¹: 3032 (–C–H– Str in aromatic), 2825(C–H Str. in –OCH₃), 1365 and 1236 (–C–O Str), 806 disubstituted aromatic ring (-para), 1630 (–CH=N, Str. azomethine group), 1667 (–C–O Str.), 2550 (–OH of –COOH group). ¹H NMR: δH (CDCl₃, 400 MHz): 3.80 (s, 3 H, –CH₃ of –OCH₃ group), 10.32 (s, 1 H, –OH group of –COOH), 8.23 (s, 1 H, –CH=N– group), 7.01–7.82 (4 H, first phenyl ring), 7.42–8.14 (4 H, second phenyl ring); Elemental analysis of C₁₅H₁₃NO₃: Calculate: C; 70.58%, H; 5.09%, O; 18.82%, N; 5.49%, Found: C; 69.62%, H; 4.96%, O; 18.74%, N; 5.42%.

Compound (2a₁₀): FT-IR (KBr) in cm⁻¹: 3031 (–C–H– Str in aromatic), 681 Polymethylene (–CH₂–)_n of –OC₁₀H₂₁, 1355 and 1230 (–C–O str), 821 disubstituted aromatic ring (-para), 1630 (–CH=N, Str. azomethine group), 1661 (–C=O Str.), 2556 (–OH of –COOH group). ¹H NMR: δH (CDCl₃, 400 MHz): 0.88 (t, 2 H, –OC₁₀H₂₁ group), 1.31 (q, 3 H, –OC₁₀H₂₁ group), 1.26–1.29 (m, 12 H, –OC₁₀H₂₁ group), 1.71 (P, 2 H, –OC₁₀H₂₁ group), 4.06 (t, 2 H, –OC₁₀H₂₁ group), 10.48 (s, 1 H, –OH group of –COOH), 8.23 (s, 1 H, –CH=N– group), 7.06–7.82 (4 H, first phenyl ring), 7.43–8.14 (4 H, second phenyl ring); Elemental analysis of C₂₄H₃₁NO₃: Calcu: C; 75.59%, H; 8.13%, O; 12.59%, N; 3.67%, Found: C; 75.32%, H; 8.02%, O; 12.52%, N; 3.62%.

Compound (2a₁₂): FT-IR (KBr) in cm⁻¹: 3032 (–C–H– Str in aromatic), 1365 and 1236 (–C–O str), 644 Polymethylene (–CH₂–)_n of –OC₁₂H₂₅, 808 disubstituted aromatic ring (-para), 1631 (–CH=N, Str. azomethine group), 1672 (–C=O Str.), 2558 (–OH of –COOH group); ¹H NMR: 0.88 (t, 2 H, –OC₁₂H₂₅ group), 1.31 (q, 3 H, –OC₁₂H₂₅ group), 1.26–1.29 (m, 14 H, –OC₁₂H₂₅ group), 1.71 (P, 2 H, –OC₁₂H₂₅ group), 4.06 (t, 2 H, –OC₁₂H₂₅ group), 10.68 (s, 1 H, –OH group of –COOH), 8.21 (s, 1 H, –CH=N– group), 7.04–7.81 (4 H, first phenyl ring), 7.43–8.14 (4 H, second phenyl ring); Elemental analysis of C₂₆H₃₅NO₃: Calcu: C; 76.28%, H; 8.55%, O; 11.73%, N; 3.42%, Found: C; 76.23%, H; 8.48%, O; 11.68%, N; 3.37%.

Compound (C₃): FT-IR (KBr) in cm⁻¹: 3032 (–C–H– Str in aromatic), 1363 and 1231 (–C–O str), 760 Polymethylene (–CH₂–)_n of –OC₃H₇, 808 disubstituted aromatic ring (-para), 1617 (–CH= N, Str. azomethine group), 1730 (–COO– group); ¹H NMR: δH (CDCl₃, 400 MHz): 0.88 (t, 3 H, –CH₃ of –OC₃H₇ group), 1.72 (t, 2 H, –OC₃H₇ group), 4.06 (t, 2 H, –OCH₂– of –OC₃H₇), 8.32 (s, 1 H, –CH=N group), 7.06–7.81 (4 H, first phenyl ring), 7.32–8.16 (4 H, second phenyl ring), 8.98 (s, 1 H, Qu-H), 8.05 (s, 1 H, Qu-H), 7.64 (d, 1 H, Qu-H), 7.60 (d, 1 H, Qu-H), 7.03 (d, 1 H, Qu-H); Elemental analysis of C₂₆H₂₂N₂O₃: Calcu: C; 76.09%, H; 5.36%, O; 11.70%, N; 6.82%, Found: C; 75.98%, H; 5.32%, O; 11.64%, N; 6.76%.

Compound (C₅): FT-IR (KBr) in cm⁻¹: 3031 (–C–H– Str in aromatic), 1365 and 1230 (–C–O str), 644 Polymethylene (–CH₂–)_n of –OC₅H₁₁, 808 disubstituted aromatic ring

(-para), 1620 (-CH=N, Str. azomethine group), 1760 (-COO- group); ^1H NMR: δH (CDCl_3 , 400 MHz): 0.88 (t, 3 H, -CH₃ of -OC₅H₁₁ group), 1.26–1.29 (m, 6 H, -OC₅H₁₁ group), 1.73 (t, 2 H, -CH₂- of -OC₅H₁₁ group), 4.06 (t, 2 H, -OCH₂- of -OC₅H₁₁), 8.31 (s, 1 H, -CH=N group), 7.06–7.83 (4 H, first phenyl ring), 7.32–8.14 (4 H, second phenyl ring), 8.98 (s, 1 H, Qu-H), 8.05 (s, 1 H, Qu-H), 7.64 (d, 1 H, Qu-H), 7.60 (d, 1 H, Qu-H), 7.03 (d, 1 H, Qu-H); Elemental analysis of C₂₈H₂₆N₂O₃: Calcu: C; 76.71%, H; 5.93%, O; 10.95%, N; 6.39%, Found: C; 76.67%, H; 5.87%, O; 10.89%, N; 6.34%.

Compound (C₁₀): FT-IR (KBr) in cm⁻¹: 3031 (-C-H- Str in aromatic), 1364 and 1236 (-C-O str), 644 Polymethylene (-CH₂-)_n of -OC₁₀H₂₁, 808 disubstituted aromatic ring (-para), 1631 (-CH=N, Str. azomethine group), 1760 (-COO group); ^1H NMR: δH (CDCl_3 , 400 MHz): 0.88 (t, 3 H, -CH₃ of -OC₁₀H₂₁ group), 1.26–1.29 (m, 12 H, -OC₁₀H₂₁ group), 1.73 (P, 2 H, -CH₂- of -OC₁₀H₂₁ group), 4.06 (t, 2 H, -OCH₂- of -OC₁₀H₂₁), 8.34 (s, 1 H, -CH=N group), 7.06–7.83 (4 H, first phenyl ring), 7.32–8.16 (4 H, second phenyl ring), 8.98 (s, 1 H, Qu-H), 8.05 (s, 1 H, Qu-H), 7.64 (d, 1 H, Qu-H), 7.60 (d, 1 H, Qu-H), 7.03 (d, 1 H, Qu-H); Elemental analysis of C₃₃H₃₆N₂O₃: Calcu: C; 77.95%, H; 7.08%, O; 9.44%, N; 5.51%, Found: C; 77.88%, H; 7.01%, O; 9.39%, N; 5.49%.

Compound (C₁₄): FT-IR (KBr) in cm⁻¹: 3031 (-C-H- Str in aromatic), 1364 and 1236 (-C-O str), 642 Polymethylene (-CH₂-)_n of -OC₁₄H₂₉, 808 disubstituted aromatic ring (-para), 1631 (-CH=N, Str. azomethine group), 1760 (-COO- group); ^1H NMR: δH (CDCl_3 , 400 MHz): 0.88 (t, 3 H, -CH₃ of -OC₁₄H₂₉ group), 1.26–1.29 (m, 14 H, -OC₁₄H₂₉ group), 1.73 (P, 2 H, -CH₂- of -OC₁₄H₂₉ group), 4.06 (t, 2 H, -OCH₂- of -OC₁₄H₂₉), 8.34 (s, 1 H, -CH=N group), 7.06–7.83 (4 H, first phenyl ring), 7.32–8.14 (4 H, second phenyl ring), 8.98 (s, 1 H, Qu-H), 8.05 (s, 1 H, Qu-H), 7.64 (d, 1 H, Qu-H), 7.60 (d, 1 H, Qu-H), 7.03 (d, 1 H, Qu-H); Elemental analysis of C₃₇H₄₄N₂O₃: Calcu: C; 78.72%, H; 7.80%, O; 8.51%, N; 4.96%, Found: C; 78.68%, H; 7.74%, O; 8.47%, N; 4.93%.

Compound (C₁₆): FT-IR (KBr) in cm⁻¹: 3031 (-C-H- Str in aromatic), 1363 and 1240 (-C-O str), 566 Polymethylene (-CH₂-)_n of -OC₁₆H₃₃, 808 disubstituted aromatic ring (-para), 1631 (-CH=N, Str. azomethine group), 1760 (-COO- group); ^1H NMR: δH (CDCl_3 , 400 MHz): 0.88 (t, 3 H, -CH₃ of -OC₁₆H₃₃ group), 1.26–1.29 (m, 18 H, -OC₁₆H₃₃ group), 1.73 (P, 2 H, -CH₂- of -OC₁₆H₃₃ group), 4.06 (t, 2 H, -OCH₂- of -OC₁₆H₃₃), 8.34 (s, 1 H, -CH=N group), 7.06–7.82 (4 H, first phenyl ring), 7.31–8.14 (4 H, second phenyl ring), 8.98 (s, 1 H, Qu-H), 8.05 (s, 1 H, Qu-H), 7.64 (d, 1 H, Qu-H), 7.60 (d, 1 H, Qu-H), 7.03 (d, 1 H, Qu-H); Elemental analysis of C₃₉H₄₈N₂O₃: Calcu: C; 79.05%, H; 8.10%, O; 8.10%, N; 4.72%, Found: C; 78.98%, H; 8.04%, O; 8.04%, N; 4.68%.

3. Result and investigation

3.1. POM investigation

The targeted compounds were synthesized by the reaction of 4-((4-n-alkoxy benzylidene) amino) benzoic acid with 8-hydroxy quinoline. In order to investigate the influence of central linkage group in presence of quinoline core on the mesophase behaviour of liquid crystalline compounds. In the present article, we have synthesized and study the effect of linking group as well as the effect of increasing alkyl chain with rigid core such as benzene and quinoline core. In present investigation, we have prepared total thirteen homologous (C₁ to C₈, C₁₂, C₁₄, C₁₆, C₁₈). The mesophase commences from early C₃ homologue. Compounds C₃ to C₇ display SmC and SmA mesophase, while compound C₈, C₁₀, C₁₂, C₁₄, C₁₆, C₁₈ display SmC as well as nematic mesophase enantiotropically manner. Odd-even effect has been observed

Table 1. Transition Temperature in °C by POM.

Sr.no	R = n-alkyl group	Transition temperatures in °C					Iso
		Cr	SmC	SmA	Nm		
1	C_1	.	—	—	—	—	164.0
2	C_2	.	—	—	—	—	158.0
3	C_3	.	108.0	.	119.0	.	152.0
4	C_4	.	104.0	.	114.0	.	148.0
5	C_5	.	102.0	.	116.0	.	140.0
6	C_6	.	98.0	.	114.0	.	142.0
7	C_7	.	81.0	.	113.0	.	138.0
8	C_8	.	74.0	.	—	92.0	126.0
10	C_{10}	.	71.0	.	—	91.0	121.0
12	C_{12}	.	68.0	.	—	88.0	116.0
14	C_{14}	.	65.0	.	—	85.0	98.0
16	C_{16}	.	61.0	.	—	82.0	94.0
18	C_{18}	.	57.0	.	—	72.0	91.0

(Cr = Solid Crystal, SmC = Smectic C phase, SmA = Smectic A phase, Nm = Nematic phase, Iso = Isotropic phase)

in Cr/M-I transition curve at C_5 to C_6 homologue in present newly synthesized series. The transition temperatures of the series are mention in below [Table 1](#).

As a preliminary investigation, the mesophases exhibited by present series were examined by using a polarising optical microscope. The samples were sandwich between a glass slide and a cover slip. C_1 to C_2 homologues in present series does not possess mesophase due to the high crystallinity and short alkyl spacer at left side chain. The nonmesomorphism of C_1 , C_2 homologue is attributed to the presence of low magnitudes of intermolecular dispersion forces and low magnitudes of dipole-dipole interactions leading to high crystallising tendency which causes abrupt to breaking the crystal lattices due to unsuitable and unfavorable magnitudes of anisotropic forces of intermolecular attractions. Thus, irregular breaking of crystal lattices and suddenly takes place at relatively higher temperature. Thus, crystalline solid state directly converted into isotropic phase without displaying any LC phase.

The phase diagram were plotted against transition temperature versus the number of carbon atoms present in n-alkyl chain in left terminal end group (-OR) is mention in below [Figure 1](#). The phase diagram shows Cr-M/I, SmC-SmA, SmA-N transition curve drawn by the linking the transition temperatures points. Cr-M/I transition curve initially decreasing as number of alkyl chain in present series is increase. Nematic mesophase commences from C_8 homologue. Nm-I transition curve shows descending tendency as increasing alkyl chain length. The SmC-SmA transition curve starts descends at C_4 homologue and then ascends to C_5 homologue this is due to the presence of odd-even parity of methylene group in n-alkyl chain length of alkoxy group. Odd-even effect is present in SmC-SmA and N-I transition curve. N-I transition curve starting with descending tendency at C_5 homologue and then continued to descending tendency upto last C_{18} homologue. It can be seen that in this homologous series the transition temperature of present synthesised series is decrease from lower

Table 2. Nematic phase of compound C_8 , C_{10} , C_{12} , C_{16} and C_{18} by miscibility method.

Sr. No.	Homologue	Texture
1	C_8	Rod type
2	C_{10}	Threaded
3	C_{12}	Rod type
4	C_{14}	Mosaic type
5	C_{16}	Threaded
6	C_{18}	Mosaic type

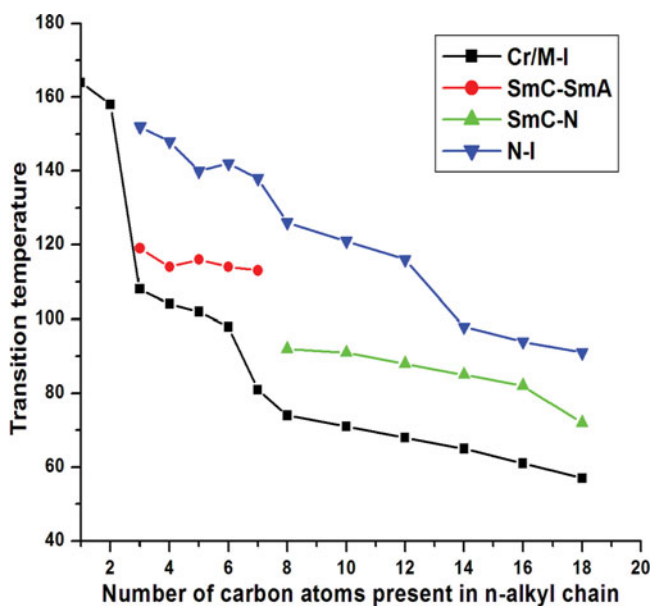


Figure 1. Phase diagram of series-1.

homologue to higher homologue, this is because of increasing the number of methylene unit $-\text{CH}_2-$ in right terminal group which increasing its chain length and causes more flexibility and polarizability. The molecular rigidity due to presence of two benzene core and third quinoline ring and presence of two central bridges are constant throughout the novel series for homologues, but the changing molecular length from homologue to homologue in the same series due to changing number of methylene units in n-alkyl 'R' chain of $-\text{OR}$ group induces flexibility. Thus changing trends in mesomorphic behaviours of a present series from homologue to homologue is attributed to the effective flexibility of each azomethine-ester linking groups based molecules in present series.

3.1.1. Nematic mesophase by miscibility method

The nematic mesophase in comp. C_8 to C_{18} were also confirmed by using miscibility method which was mention in below Table 2. Comp. C_{10} shows threaded type nematic phase whereas in comp. C_{12} , rod type textural image was seen. Comp. C_{14} homologue shows rod type textural pattern of nematic phase. Comp. C_{16} to C_{18} shows threaded type textural pattern of nematic mesophase.

3.1.2. Textural study

The solid samples held between an untreated glass slide and a coverslip were heated to their isotropic phase and cooled slowly. As shown in Figure 2, a threaded type line textural image of nematic phase of compound C_{10} seen at 71.0°C on cooling condition. Compound C_{18} displays rod type textural pattern of SmA phase at 116.0°C on cooling condition. Compound C_6 shows rod type textural pattern of SmA phase at 114.0°C on cooling condition while in compound C_{14} , a mosaic type textural image of nematic phase observed at 72.0°C on cooling condition. It can be noted that higher member of series displayed nematic mesophase as compare to lower membered of the series. The nematic mesophase is attributed to the suitable magnitudes of end to end intermolecular anisotropic forces of attractions and closeness as a consequence of favorable molecular rigidity, linearity due to the presence linking group and flexibility cause

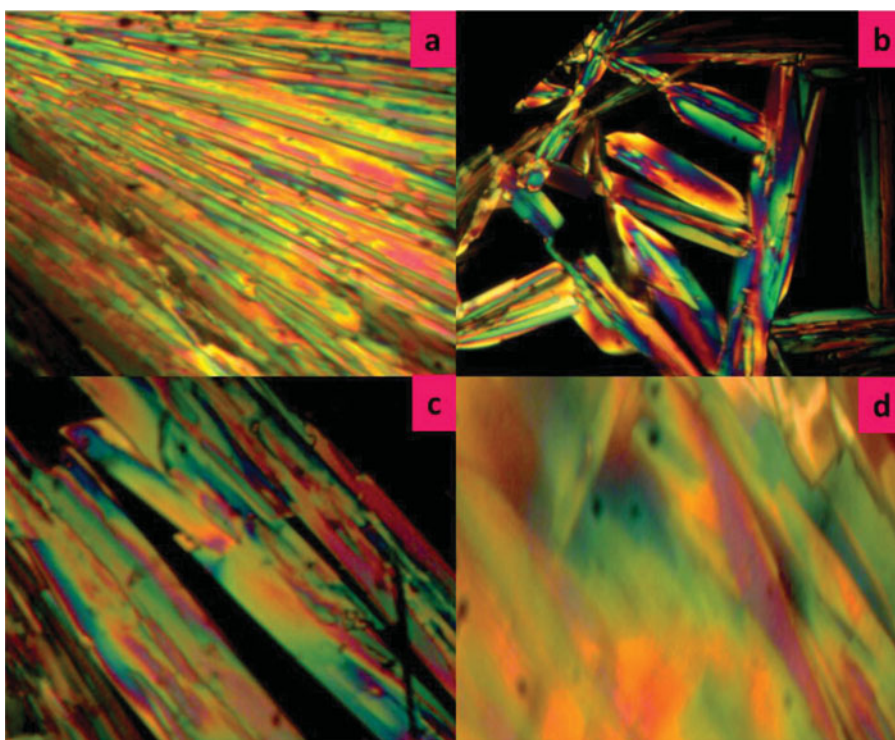


Figure 2. Microphotographs of the optical textural pattern (a) threaded line type texture image of compound C_{10} , (b) SmA phase of compound C_4 ; (c) SmA phase of compound C_6 and (d) mosaic type textural pattern of comp. C_{14} .

by the presence of left side chain generate permanent dipole moment across the long molecular axis, suitable magnitudes of dispersion forces and dipole-dipole interactions, molecular polarizability and polarity which facilitate the molecules under microscopic study to float on the surface with statically parallel orientational order within certain range of temperature as nematic phase [25].

3.1.3. Comparative study and thermal stability

In order to examine the effect of schiff base ($-\text{CH}=\text{N}-$) linkage group, the LC behaviour of present synthesized series-1 was compared with structurally similar reported series-2 as shown in Figure 3. Homologous series-1 and X are identical with respect to three phenyl

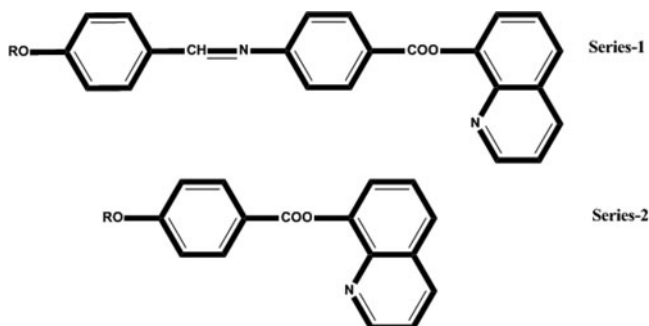


Figure 3. Structurally comparison with previously reported series.

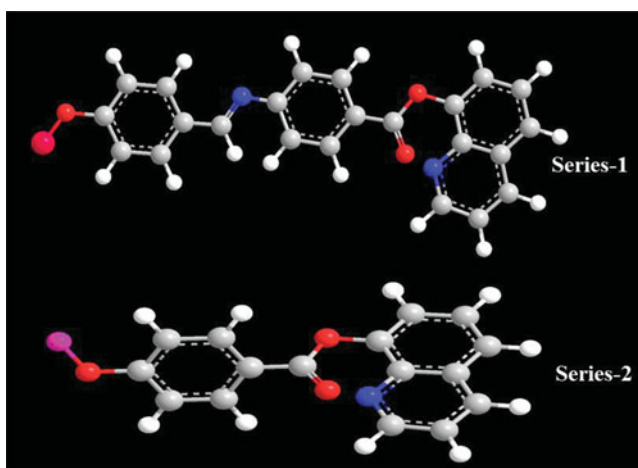


Figure 4. Ball-stick model of series-1 and series-2.

rings, two central bridges joining phenyl rings and two flexible terminal end groups (-OR and $-\text{OC}_{16}\text{H}_{33}$). But, they differ with respect to their geometrical shapes linear and nonlinear respectively for the same homologues from series to series. Therefore they differ with respect to combined effects of molecular rigidity and flexibility, including intermolecular distance and molecular polarizability which operates LC behaviours of series. Homologous series-2 are identical with series-1 at second ester linkage group and quinoline ring at terminal side. Series-2 display nonliquid crystalline behaviour. The molecular length of series-2 is lower as compare to series-1. Introducing of azomethine ($-\text{CH}=\text{N}-$) linkage group in series-1 which increase the length of molecules as compare to series-2 causes mesomorphism with good thermal stability. Thus, mesomorphic (LC) properties are attributed to the magnitudes of differing features like geometrical shapes, molecular rigidity and flexibility of molecules. **Figure 4** represents the ball-stick model which indicates the geometrical shape and molecular length of series-1,-2.

Table 3 shows the average thermal stabilities and mesophase range of newly homologous Series (C_1 to C_8 , C_{10} , C_{12} , C_{14} , C_{16} , C_{18}). The N-I thermal stability of Series is 107.66°C . The SmC-SmA thermal stability is 115.2°C . Thermal stability of SmC-N phase is 85.0°C . However, the SmA-I thermal stability of Series is 144.0°C . The average mesophase length of present series is 44.0°C and 34.0°C respectively. The thermal stability of SmA-I and SmC-SmA phase is higher than the thermal stability of N-I and SmC-N phase. The ester linking group favors the lamellar packing due to the dipole-dipole interaction which ultimately generated the smectic phase [26].

Table 3. Average thermal stability in $^\circ\text{C}$.

Series	Series-1	Series-2
SmC-SmA	115.2	—
SmC-N	85.0	—
Commencement of SmC phase	C_3	—
SmA-I	144.0	—
Commencement of SmA phase	C_3	—
N-I	107.66	—
Commencement of Nematic phase	C_8	—
Degree of mesomorphism in $^\circ\text{C}$ from minimum to maximum	44.0 to 34.0	—
	C_3 C_{18}	

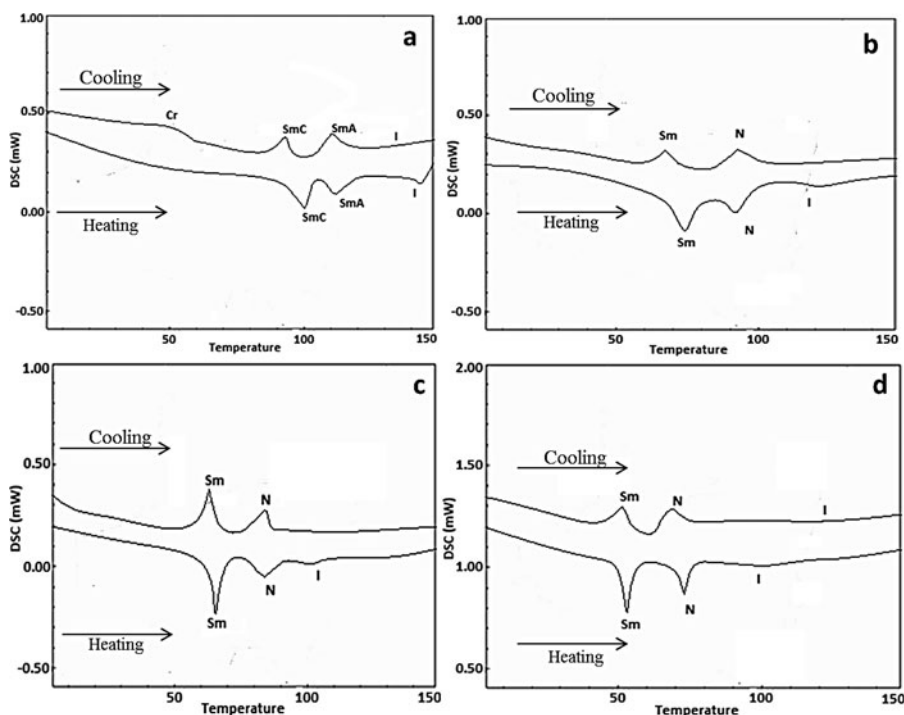


Figure 5. DSC thermogram of (a) C_5 , (b) C_8 , (c) C_{12} and (d) C_{18} homologue.

3.2. DSC analysis

DSC is a valuable method for detecting phase transitions. The thermal behaviour of novel homologues series were confirmed by DSC analysis shown in below [Figure 5](#). Thermogram is traces in both heating and cooling condition. Microscopic transition temperature values are similar to the DSC data.

On heating condition, C_5 homologue shows two endothermic peaks on heating and cooling condition. The traced two endothermic peaks correspond to the SmC and SmA phase. First endothermic peak observed at 101.12°C , which indicates the presence of SmC phase. While second endothermic peak observed at 113.51°C to confirmed the changing of SmC phase into SmA phase. On cooling condition, again two endothermic peaks traced at 96.51°C and 114.82°C , which was further confirmed by using POM study. Comp. C_8 shows two significant peaks on heating and cooling condition. First endothermic peak is observed at 74.08°C and second endothermic peak trace at 92.73°C on heating condition. While on cooling condition, two endothermic peaks observed at 69.93°C and 95.84°C . Comp. C_{12} shows two endothermic peaks at 66.91°C and 86.98°C on heating condition while, on cooling condition two endothermic peaks traced at 64.22°C and 88.23°C . For comp. C_{18} , two endothermic peaks trace on heating and cooling condition. On heating condition first two endothermic peaks trace at 53.28°C and 72.37°C while on cooling condition, it traced at 52.85°C and 71.34°C to indicates the presence of SmC and nematic mesophase which was confirmed by POM analysis.

Transition temperature obtained by DSC analysis at heating and cooling condition and the value of enthalpy and entropy is mention in [Table 4](#). Molecules of every homologue randomly oriented in all possible directions with high order of disorder or entropy ($\Delta S = \Delta H/T$) beyond isotropic temperature and the enthalpy value (ΔH). But, at cooled condition, the same from

Table 4. Transition temperature (°C) and enthalpy (J g⁻¹) and entropy change (J g⁻¹k⁻¹) by DSC measurement.

Homologuesor Comp.	Transition	Heating scan(°C)	Cooling scan(°C)	ΔH (-Jg ⁻¹)	ΔH (Jg ⁻¹)	ΔS (J g ⁻¹ k ⁻¹)	ΔS (J g ⁻¹ k ⁻¹)
C₅	Cr-SmC	101.12	96.51	3.17	8.26	0.0084	0.0223
	SmC-SmA	113.51	114.82	15.24	12.67	0.0394	0.0326
	SmA-I	>140.0	—	8.10	—	0.0196	—
C₈	Cr-SmC	74.08	69.93	7.92	6.90	0.0228	0.0201
	SmC-N	92.73	95.84	12.21	9.45	0.0333	0.0256
	N-I	>126.0	—	4.34	—	0.0108	—
C₁₂	Cr-SmC	66.91	64.22	8.22	4.54	0.0241	0.0134
	SmC-N	86.98	88.23	18.16	12.98	0.0504	0.0359
	N-I	>116.0	—	3.43	—	0.0081	—
C₁₈	Cr-SmC	53.28	52.85	2.29	7.43	0.0068	0.0228
	SmC-N	72.37	71.34	12.53	8.54	0.0362	0.0248
	N-I	>92.0	—	4.62	—	0.0126	—

and below isotropic temperature, the mesophase is persisted to appear reversibly at high or lower temperature at observed during heating and cooling condition. The enthalpy values also indicate the crystal to mesophase and mesophase to isotropic transition in compounds C₅, C₈, C₁₂ and C₁₈. The mesophase observed enantiotropically manner in present series.

4. Conclusion

In this article, we have presented the synthesis and characterization as well as the mesomorphic behaviour quinoline based homologues series viz. quinoline-8-yl-4-((4-n-alkoxy benzylidene) amino) benzoate (**n = 1 to 8, 10, 12, 14, 16, 18**), which comprised of Schiff base ester moieties as linking group and alkoxy side chain group. The synthesized compounds with having short alkyl spacer exhibits SmC and SmA phases, while in long alkyl spacer compounds exhibits SmC and N mesophases. An additional feature found in the present series is that the presence of azomethine (-CH=N-) and ester (-COO-) group as a central part and terminally quinoline core leads more thermal stable mesophase.

Acknowledgement

Authors acknowledge thanks to Dr. R.R.Shah, principal and management of K. K. Shah Jarodwala Maninagar Science College, Ahmedabad. Authors are also thankful to NFDD Centre for providing analytical and spectral services.

References

- [1] Macros, M., Omenat, A., Serrano, J. L., & Ezcurra, A. (1992). *Adv.Mater.*, 4, 285.
- [2] Hird, M., Toyne, K. J., & Gray, G. W. (1993). *Liq.Cryst.*, 14, 741.
- [3] Hird, M., Toyne, K. J., Gray, G. W., Day, S. E., McDonnell, D. G. (1993). *Liquid Crystal.*, 15, 123.
- [4] Lauk, U., Scrabol, P., & Zollinger, H. (1983). *Helv.Chim.Acta.*, 66, 1574.
- [5] Sierra, J., Serrano, J. L., Ros, M. B., Ezcurra, A., & Zubia, J. (1992). *J.Am.Chem.Soc.*, 114, 7645.
- [6] Zuniga, C., Belmar, J., Parra, M., Ramirez, A., Decap, J., Ros, B., & Serrano, J. L. (1996). *Liquid Crystals.*, 20, 253.
- [7] Leardini, R., Nanni, D., Pedulli, G. F., Tundo, A., & Zanardi, G. (1987). *Liq.Cryst.*, 2, 625.
- [8] Zuniga, C., Bartulin, J., Muller, H. J., Schumacher, E., & Taylor, T. R. (1991). *Mol.Cryst.Liq.Cryst.*, 206, 131.

- [9] Zuniga, C., Belmar, J., Parra, M., Ramirez, A., Decar, J., Ros, B., & Serano, J. L. (1996). *Liq. Cryst.*, 20, 253.
- [10] Lin, H. C., Lai, L. L., Hsieh, W. P., & Huang, W. Y. (1997). *Liquid Crystal*, 22, 661.
- [11] Zanardi, G. (1987). *Liquid Crystal*, 2, 625.
- [12] Chia, W. L., & Cheng, Y. W. (2008). *Heterocycles*, 75, 375.
- [13] Chia, W. L., Chia, W. L., & Chang, C. H. (2009). *Mol. Cryst. Liq. Cryst.*, 506, 47.
- [14] Chia, W. L., Liao, K. H., & Ho, C. I. (2009). *Liq. Cryst.*, 36, 557.
- [15] Chia, W. L., Ye, F. J., & Chen, E. C. (2013). *Liquid Crystals*, 40, 989.
- [16] Bhoya, U. C., Vyas, N. N., & Doshi, A. V. (2012). *Mol. Cryst. Liq. Cryst.*, 552, 104.
- [17] Lava, K., Evrard, Y., Hecke, K. V., Meervelt, L. V., & Binnemans, K. (2012). *RSC Advance*, 2, 8061.
- [18] Ha, S. T., Ong, L. K., Wong, J. P. W., Yeap, G. Y., Lin, H. C., Ong, S. T., & Koh, T. M. (2009). *Phase Transition*, 82, 387.
- [19] Yeap, G. W., Ha, S. T., Lin, P. L., Ito, M. M., & Sanehisa, S. (2004). *Mol. Cryst. Liq. Cryst.*, 423, 73.
- [20] Dave, J. S., Kurian, G. (1997). *Mol. Cryst. Liq. Cryst.*, 175, 42.
- [21] Yelamaggad, C. V., Mathews, M., Negamani, A., Rao, S., Prasad, S. K., Findeisen, S., & Weissflog, W. (2007). *J. Mater. Chem.*, 17, 284.
- [22] Sharma, V. S., & Patel, R. B. (2016). *Mol. Cryst. Liq. Cryst.*, 630, 58.
- [23] Furniss, B. S., Hannford, A. J., Smith, P. W. G., & Tatchell, A. R. (Revisors). (1989). *Vogel's Text-book 245 of Practical Organic Chemistry* (4th ed.), 563, Longmann Singapore Publishers Pvt. Ltd., Singapore.
- [24] Uhood, J. A. (2011). *International Journal of Molecular Science*, 12, 3182.
- [25] Suthar, D. M., & Doshi, A. V. (2013). *Mol. Cryst. Liq. Cryst.*, 571, 1.
- [26] Gray, G. W. (1962). *Molecular Structure and Properties of Liquid Crystals*, Academic Press, London.